A COVID-19 Based on Fractional Order Integral-Tilt Derivative Controller for Nonlinear Servomechanism Model

MOHAMED A. SHAMSELDIN[1], MAHMOUD SALAH[2], ABDEL GHANY MOHAMED[3]
M.A. ABDEL GHANY[4]
[1]Mechanical Engineering Department, The Egyptian Chinese University, Cairo, EGYPT,
[2]Electric Engineering Department, Faculty of engineering, Helwan University, Cairo, EGYPT,
[3] Electrical Engineering Department, Higher Engineering Institute, Thebes Academy, Cairo, EGYPT
[4]Electrical Engineering Department, October 6 University, Cairo, EGYPT

Abstract: - In this research, a new one-axis servomechanism investigation is presented, taking into account parameter fluctuation and system uncertainty. Additionally, a novel method for very effective TID control was created to accurately monitor a chosen profile. A comparative study between the suggested control method and the well-known controllers (PID and Nonlinear PID) is also included. The COVID-19 optimization technique was used to discover the best control parameters. Through the online simulation, the servomechanism system's settings were modified at random within a predetermined range. As nonlinearity resources (friction, backlash, environmental influences), these parameters fluctuate and contribute to system uncertainty. It had been completed and looked at to compare the linear and nonlinear models. The results demonstrate that the suggested controller is capable of tracking the number of operational points with high accuracy, a short rising time, and little overrun.

Key-Words: - COVID-19 optimization; PID control; Servomechanism; Uncertainty; Nonlinear systems.

Received: November 29, 2022. Revised: August 28, 2023. Accepted: September 26, 2023. Published: November 6, 2023.

1 Introduction

For servomechanism systems, the parameters of the friction and backlash models are often unknown, leading to system uncertainty.

There are many control approaches for single-axis controllers, including standard PID control, self-tuning PID control, fuzzy PID control, adaptive control, and sliding mode control and so on [1].

Several nonlinear systems respond satisfactorily to the standard PID controller, but it performs poorly when there is uncertainty and parameter change [2]. In order to achieve a good response for typical applications (pick and place jobs or low accuracy movements), the majority of industrial applications use conventional PID control [3].

The fuzzy logic system is a useful tool for dealing with nonlinearity and uncertainty problems in complex systems [4]. However, it requires a lot of data and a fast processor. Also, the neural network also requires a significant amount of training time and data storage [5];[6].

The sliding mode technique has the advantage that it provides strong tracking performance over a variety of position command operating locations. On the other hand, chattering phenomena can make it challenging to improve control accuracy and, in uncommon circumstances, can result in system instability [7];[8].

Currently, the complicated system needs a controller with simple structure to minimize the memory size and reducing the cycle time. Moreover, it can achieve a satisfied performance and absorbing the system uncertainty and nonlinearity [9];[10]. So, the researches develop the PID control with linear fixed parameters to nonlinear PID control which contain a nonlinear function. So, it gives a compromise solution where the structure of controller still simple and the performance had been improved [11]. By comparison, the nonlinear PID controller and the advanced control techniques which have a complex structure still the advanced control techniques give a smooth, fast, and robust performance [12]; [13]; [14].

This paper seeks to develop a new Fractional Order Integral-Tilt Derivative (FOITD) Controller optimized by a COVID-19 optimization which has a simple structure and can achieve a smooth and fast response close to the advanced control techniques. The proposed technique investigated by a comparative study with the PID control and nonlinear PID control. Also, the nonlinearity resources like friction and backlash are treated by the suggested control strategy. Additionally, it can handle the uncertainty issue without requiring a sophisticated friction and back-lash model.

The paper is prepared as following, firstly, the system modelling is presented. Secondly, the

proposed control techniques are demonstrated. Thirdly, the results are illustrated. Finally, the conclusion is discussed.

2 System Modeling

The nonlinear single-axis model with uncertainty is demonstrated in this section. The proposed model was created to mimic the nonlinearity and unpredictability that actually exist. Uncertainty can be defined in this study as the unpredictable change in system parameters. The single-axis servomechanism's general structure is depicted in Figure 1.

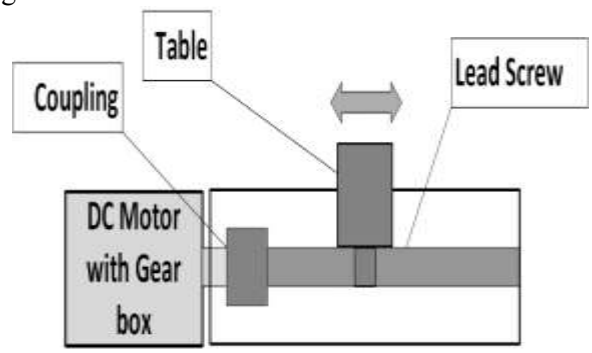

Fig. 1. One axis servomechanism system.

The system parameters will be modified at random online in order to emulate the servomechanism's uncertainty and nonlinearity. For instance, the online variables ϵ_g, ε_e and σ will be continuously modified to mimic the backlash behaviour. Additionally, the μ_{gf}, μ_b and ϱ will fluctuate randomly within a predetermined range in order to mimic the friction behavior. Additionally, the W_a and D_a will be changed at random to implement the motor uncertainty. The values of the system parameters and the change boundaries are displayed in table 1 below.

The following Figure 2 demonstrates the simulation of the backlash effect by changing the gear ratio randomly online. Also, the rest of the parameters in table 2 change online such as the gear ratio parameter.

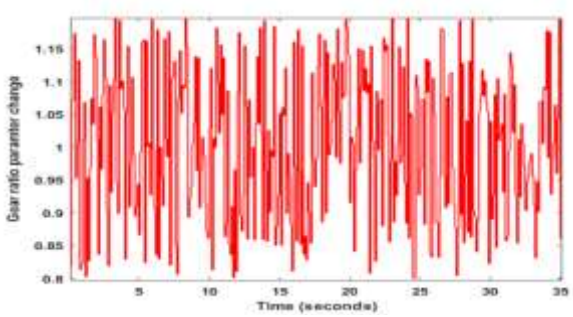

Fig. 2. Gear ratio uncertainty.

Table 1. Variable parameters of the servomechanism system.

Parameter	**Unit**	**Definition**	**Borders of change**
σ=0.00508	m/rev	Pitch of feed screw	0.005~ 0.0051
ϵ_g=1	------	Gear reduction ratio	0.8~ 1.2
Da=0.5	ohm	Motor winding resistance	0.45~ 0.55
ε_m=2.373× 10-3	Kg.m2	Motor shaft inertia	2.3×10-3~ 2.4×10-3
ϱ = 0	Nm/(rad/sec)	Viscous damping ratio	0.00001~ 0.00002
μ_{gf} = 0.1	-----	Friction coefficient in guides	0.95~ 0.15
μ_b= 0.005	------	Bearings Friction coefficient	0.0045~ 0.0055

The following table 2 demonstrates the fixed parameters of servomechanism system.

Table 2. Constant parameters of the servomechanism system.

Parameter	Unit	Definition
mt=180	kg	table mass
mw=200	kg	max mass workpiece
mL=8.15	kg	leadscrew mass
dp=0.0445	m	Feed screw diameter
fz=2000	N	max vertical force
Ff=8000;	N	max feeding force
Fp=5000	N	preload force in thrust bearing
f=0.170	N	rapid traverse velocity m/s
tr=0.1	sec	servo rise time sec
X_a=220	V	Motor rated voltage

In Figure 3, the input voltage motor which changes continuously as a sin form. The corresponding output stage position of the servomechanism is shown as Figure 4. It can be noted the effect of uncertainty and nonlinearity of stage position output.

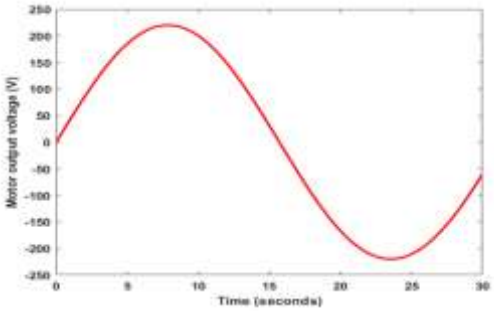

Fig. 3. The input voltage for DC motor.

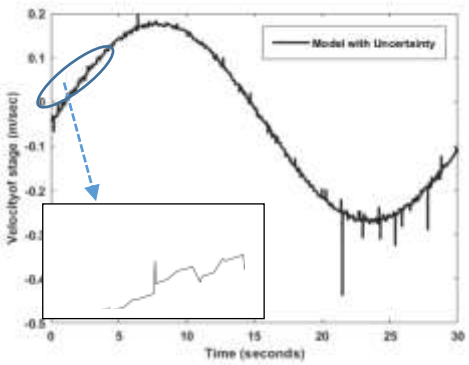

Fig. 4. The corresponding output position of servomechanism.

3 Control Techniques

3.1 PID Control

PID controllers have been applied for control of various dynamical systems ranged from industrial process to complicated dynamics such as ship and aircraft [3].
The transfer function of the PID controller is $K(s) = K_P + \frac{K_i}{s} + K_d s$. Where K_p, K_i, k_d are proportional, integral and differential gains respectively [16]. In this paper the COVID-19 optimization technique will be used to obtain the optimal values of PID controller parameters. The initial population will be built as shown in equation (1).

$$\text{P1} = \begin{bmatrix} K_{p1} & K_{i1} & K_{d1} & F_1 \\ K_{p2} & K_{i2} & K_{d2} & F_2 \\ .. & .. & .. & .. \\ .. & .. & .. & .. \\ K_{pn} & K_{in} & K_{dn} & Fn \end{bmatrix} \quad (1)$$

Where n is the number of patients and the values F is corresponding immunity.

3.2 Nonlinear PID (NPID) Control

In order to improve the performance of linear PID controllers, many techniques have been established to increase the adaptability and robustness by adopting the self-tuning method, general predictive control, neural networks strategy and fuzzy logic, and other methods [17].

The NPID controllers have the advantage of high initial gain to achieve a fast response, followed by a low gain to avoid an oscillatory behavior. In this study, a performance enhancement to the conventional linear PID controller is proposed by combining a sector-bounded nonlinear gain into a linear fixed gain PID control architecture.

The proposed enhanced nonlinear PID (NPID) controller consists of two parts. The first part is a sector bounded nonlinear gain $K_n(e)$ while, the second part is a linear fixed-gain PID controller (Kp, Ki and Kd). The nonlinear gain $K_n(e)$ is a sector-bounded function of the error e (t). The previous researches have been made where the nonlinear gain $K_n(e)$ has a one scalar value.

In this paper, The $K_n(e)$ acts as a row vector can expressed as $K_n(e) = [K_{n1}(e) \quad K_{n2}(e) \quad K_{n3}(e)]$ which will be enhanced the NPID controller.
The proposed form of NPID control can be described as follows.

$$u(t) = K_p[K_{n1}(e).e(t)] + K_i \int_0^t [K_{n2}(e).e(t)]\,dt + K_d\left[K_{n3}(e).\frac{de(t)}{dt}\right] \quad (2)$$

Where $K_{n1}(e), K_{n2}(e)\ and\ K_{n3}(e)$ are nonlinear gains. The nonlinear gains represent any general nonlinear function of the error e which is bounded in the sector $0 < K_n(e) < K_n(e)\text{max}$.
There is a wide range of choices available for the nonlinear gain $K_n(e)$. One simple form of the nonlinear gain function can be described as.

$$K_{ni}(e) = ch(w_i e) = \frac{\exp(w_i e)+\exp(-w_i e)}{2} \quad (3)$$

Where $i = 1, 2, 3.$

$$e = \begin{cases} e & |e| \le e_{max} \\ e_{max} sgn(e) & |e| > e_{max} \end{cases} \quad (4)$$

Where w_i and e_{max} are user-defined positive constants. The nonlinear gain $K_n(e)$ is lower bounded by $K_n(e)$min = 1 when e = 0, and upper-bounded by $K_n(e)$max = ch($w_i\, e_{max}$). Therefore, e_{max} stand for the range of deviation, and w_i describes the rate of variation of $K_n(e)$.
The population in each generation is represented by matrix as given by (5). Each row represents a one patient that include $K_P,\ K_i,\ K_d, w_1, w_2\ and\ w_3$ values and the last column is added to adapt fitness values (F) of corresponding immunity.

$$P_3 = \begin{bmatrix} K_{p1} & K_{i1} & K_{d1} & w_{11} & w_{21} & w_{31} & F_1 \\ K_{p2} & K_{i2} & K_{d2} & w_{12} & w_{22} & w_{32} & F_2 \\ .. & .. & .. & .. & .. & .. & .. \\ .. & .. & .. & .. & .. & .. & .. \\ K_{pn} & K_{in} & K_{dn} & w_{1n} & w_{1n} & w_{3n} & Fn \end{bmatrix} \quad (5)$$

Where n is the number of patients.

3.3 TID Control

PI and PID linear controllers are two examples of the many types of linear controllers that can be used to meet control objectives, which are primarily defined by the steady-state and transient needs [18]. In each application, tilt integral derivative (TID) controllers are chosen because they are easier to tune, have a higher disturbance rejection ratio, and have fewer effects on closed loop response from changes in plant parameters. Figure 5 depicts the TID controller's structural layout.

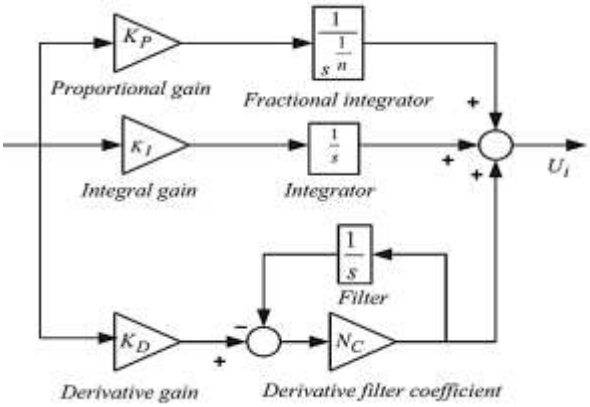

Fig. 5. Structure of TID controller [18].

The proportional component of the controller is replaced with tilted component having a transfer function $s^{\frac{-1}{n}}$. In Figure 5, K_P, K_D, K_I are proportional, derivative, integral gains and n is a nonzero real number respectively. The parameter NC is the derivative filter coefficient. The mathematical model of TID controller is given by:

$$TF_{TID} = \frac{K_t}{s^{\frac{1}{n}}} + \frac{K_I}{s} + K_D\left(\frac{N_C s}{s+N_C}\right) \quad (6)$$

3.4 COVID-19 optimization

In this section the COVID-19 optimization steps will be demonstrated. The following Figure 6 shows the online tuning system for the COVID-19 optimization.

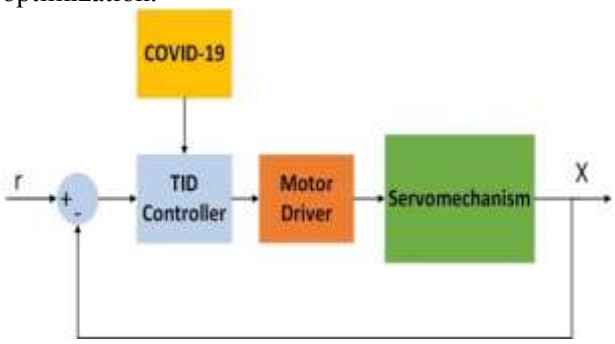

Fig. 6. The online tuning system for the TID control.

The COVID-19 optimization algorithm, which is a new and powerful optimization technique introduced in this study, is used to identify the ideal controller parameters according to the output response behavior and the required performance. The goal of this part is to choose the controller's parameters' ideal values.
The creation of the initial population is the first step. There are no patients in the initial population. It contains m columns (number of controller parameters) and n rows (number of solutions). As in the COVID-19 epidemic scenario, it recognizes the first human being infected.
Several cases may be taken into consideration in the second step, where the propagation of the disease is dependent on how the population matrix (zero patient) behaves. In the first instance, some of the sick people pass away. According on the COVID-19 virus fatalness rate, death is a probability. Such people can no longer spread the infection to new people. The second instance is when those who have the COVID-19 virus will spread it to new people (intensification). According to a certain likelihood, two methods of disease transmission are therefore taken into consideration. If the COVID-19 virus is spreading rapidly, infected people will infect new people according to the COVID-19 virus super spreading rate rather than the pace of spreading as it does for ordinary spreaders. Ordinary people and super-spreaders can follow directions and come up with answers in quite different ways. People are

therefore likely to travel, making it possible for them to disseminate the disease to settings that may be very different.

The third step, population modernization: Each generation updates three populations that have been preserved. Number of deceased: If anybody passes away, their death is added to this population and is permanently lost. Recovered population: Following each repetition, infected people are sent to the recovered population after propagating the COVID-19 virus in accordance with the preceding phase. The likelihood of reinfection is well understood. So, if a member of this population meets the criteria for reinfection, they could become infected again at any iteration.

As people are capable of isolating themselves while acting out social distancing techniques, another condition needs to be measured. When an isolation probability is met, it is assumed for simplicity that an isolated person is also sent to the recovered population.

Lately, a population with a recent infection: Every sick person from each iteration is collected into this population using the method outlined in the preceding phases. At each repetition, it's feasible that additional infected people be produced repeatedly and thereafter.

Before the following iteration begins, it is advised to remove these recurrent offenders from the population. The employment of vaccines as an objective function that can treat the afflicted population is taken into consideration.

Halt criterion is the fourth action. The capacity of the suggested method to run to completion without requiring any parameter control is one of its most crucial aspects. Because the recovered and dead populations are constantly growing over time and the newly infected population is unable to spread infection, this situation arises. According to estimates, after a given number of iterations, the population of infected people grows. The healthier and lifeless populations are too large, and the size of the sick population falloffs over time, so starting with a certain iteration, the newly sick population will be lower than the one that is already present.

In agreement with the objective COVID-19 function in equation, the effectiveness of each row will be examined (8). Poor performance identifies the susceptible to death afflicted population. However the strong result suggests that COVID-19 antivirus has recovered its population.

$$\forall_t = (\forall_1 + \forall_2 + \forall_3 + \forall_4)/4 \quad (7)$$

$$\forall_1 = \frac{|t_r - t_{rd}|}{t_{rd}} \quad (8)$$

$$\forall_2 = \frac{|t_s - t_{sd}|}{t_{sd}} \quad (9)$$

$$\forall_3 = \frac{|e_{ss} - e_{ssd}|}{e_{ssd}} \quad (10)$$

$$\forall_4 = \frac{|OS - OS_d|}{OS_d} \quad (11)$$

Where (t_{rd}) is the chosen rise time and (t_r) is the calculated rise time, (OS_d) is the preferred maximum overshoot and (OS) is the actual overshoot, (t_{sd}) is the wanted settling time and (t_s) is the dominant settling time and (e_{ssd}) is the favorite equilibrium error and (e_{ss}) is the estimated equilibrium error.

Four sub-objective functions can be used to illustrate how the objective function works to meet the needs of the designer. The first sub-objective function places a strong emphasis on accelerating the rising time of the entire EV drive system. Trying to shorten the settling time is the second sub-objective function. The steady-state error is quantified by the third sub-objective. Investigating the necessary overshoot is the fourth sub-objective function. Each sub-objective COVID-19 function has a value that ranges from zero to one. In other words, the inclusive objective COVID-19 function considered the middling of the total of the four sub-objective functions.

The obtained parameters can be abridged in the following table 3.

Table 3. The obtained parameters of the servomechanism system.

PID	K_P= 25.33		K_I=0.125		K_D=56.25	
TID	K_P= 10.35		K_I=0.0256	K_D=86.26		N= 0.21
NPID	K_P= 0.34	K_I= 0.25	K_D= 0.012	W1 = 0.289	W2 = 18.25	W3 =0.152

4 Results and Discussion

For test one (step operating point), Figure 7 shows a comparison of the PID control, NPID control, and suggested TID control. Among other techniques, the TID control has a low rise time, there are no variations around the reference point in the proposed TID control compared to other techniques and there is a small overshoot respect to the NPID control.

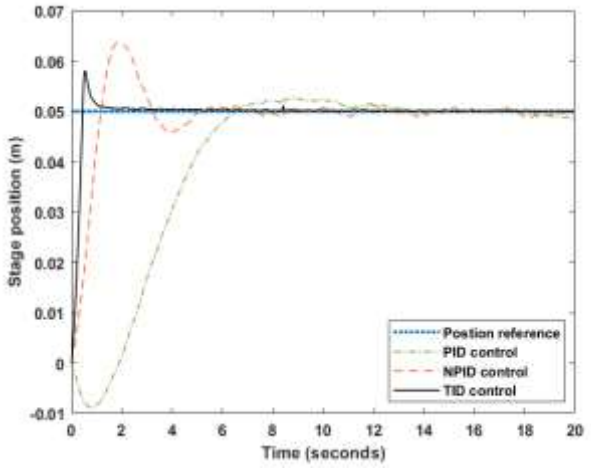

Fig. 7. The stage position response for each controller at step reference.

Figure 8 demonstrates the corresponding controller output. It is demonstrated that the TID controller has a high starting value. Also, it has a high shuttering to can absorb the system uncertainty. Moreover, the output of the TID controller increases and decreases quickly in a short time at the beginning of the test to respond to the system as fast as possible.

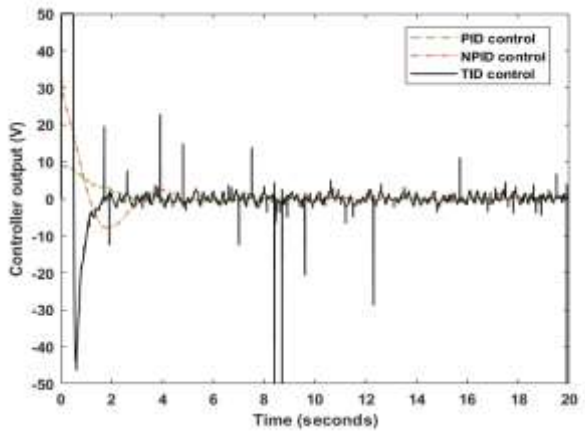

Fig. 8. The corresponding controllers output at step reference.

The results of the control strategies for the second test (stair operating point) are shown in Figure 9. The TID control's excellent accuracy in tracking and following the operating point's constant change is demonstrated. PID and NPID controllers experience a significant delay as compared to TID controllers.

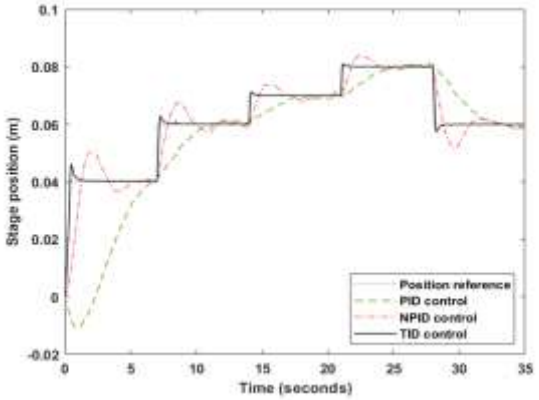

Fig. 9. The stage position response for each controller at stair reference.

The corresponding controller output for the continuous change of operating point test is shown in Figure 10. The high beginning value of the TID controller at each new operating point is demonstrated. Additionally, because TID controller output changes more quickly than PID and NPID controllers do, it can properly track the position reference and take into account system uncertainty.

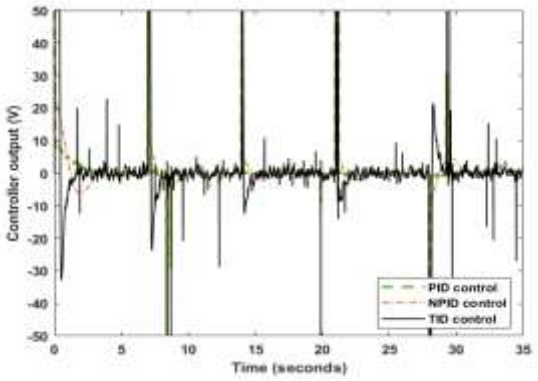

Fig. 10. The corresponding controllers output at stair reference.

The robustness of the proposed controller is tested by applying operating point as continuously changing in sinusoidal form. Figure 11 shows that the stage position is oscillated as the reference. It can be noted that the TID control can absorb the system uncertainty where it track the reference profile accurately. While the other control techniques (PID and NPID) have a poor tracking and high delay compared to the reference profile.

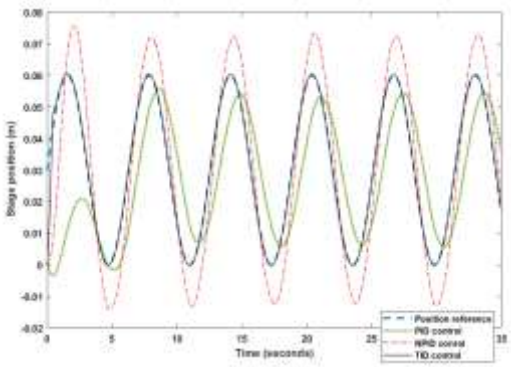

Fig. 11. The stage position response for each controller at sin function reference.

The corresponding controller output for the sin reference profile test is shown in Figure 12. The output of each controller fluctuates continuously to adapt with the reference profile. Also, it can be noted that the TID control has a high noise to can absorb the system uncertainty and nonlinearity.

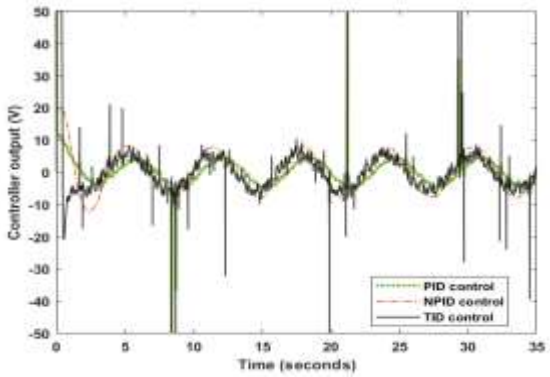

Fig. 12. The corresponding controllers output at sin function reference.

References:

[1] Abdelfattah, Hany, Said A Kotb, Mohamed Esmail, and Mo-hamed I Mosaad. 2023. "Adaptive Neuro-Fuzzy Self-Tuned-PID Controller For." International Journal of Robotics and Control Systems 3 (1): 1–18.

[2] Abeykoon, Chamil. 2016. "Single Screw Extrusion Control: A Comprehensive Review and Directions for Improvements." Control Engineering Practice 51: 69–80.https://doi.org/10.1016/j.conengprac.2016.03.008.

[3] BOUSSAADA, Mohamed, Riadh ABDELATI, Hajer LAHDHIRI, and Hedi YAHIA. 2023. "PV Characterization and MPPT Based on Characteristic Impedance Using Arduino Board and MATLAB Interface." Studies in Informatics and Control 32 (1): 91–100. https://doi.org/10.24846/v32i1y202309.

[4] Daraz, Amil, Suheel Abdullah Malik, Ahmad Taher Azar, Sher-az Aslam, Tamim Alkhalifah, and Fahad Alturise. 2022. "Optimized Fractional Order Integral-Tilt Derivative Controller for Frequency Regulation of Interconnected Diverse Renewable Energy Resources." IEEE Access 10: 43514–27. https://doi.org/10.1109/ACCESS.2022.3167811.

[5] FAYTI, Majid, Mostafa MJAHED, Hasan AYAD, and Abdeljalil El KARI. 2023. "Recent Metaheuristic-Based Optimization for System Modeling and PID Controllers Tuning." Studies in In-formatics and Control 32 (1): 57–67. https://doi.org/10.24846/v32i1y202306.

[6] IBRAHIM, Motaz Musa, Lei MA, Yiming ZHAO, and Haoran LIU. 2023. "Robust Direct Current Control of Single-Phase PWM Rectifiers Based on a Mixed H2/H∞ Controller." Studies in Informatics and Control 32 (1): 81–90. https://doi.org/10.24846/v32i1y202308.

[7] Ma'arif, Alfian, and Abdullah Çakan. 2021. "Simulation and Arduino Hardware Implementation of Dc Motor Control Using Sliding Mode Controller." Journal of Robotics and Control (JRC) 2 (6): 582–87. https://doi.org/10.18196/jrc.26140.

[8] Madiouni, Riadh. 2018. "Robust PID Controller Design Based on Multi-Objective Particle Swarm Optimization Approach." Proceedings - 2017 International Conference on Engineering and MIS, ICEMIS 2017 2018-Janua: 1–7. https://doi.org/10.1109/ICEMIS.2017.8273039.

[9] Mohamed A. Abdel Ghany, Mohamed A. Shamseldin. 2023. "Fuzzy Type Two Self-Tuning Technique of Single Neuron PID Controller for Brushless DC Motor Based on a COVID-19 Optimization Mohamed." International Journal of Power Elec-tronics and Drive Systems 14 (1).

[10] Mohamed A. Shamseldin, Abdel Halim M. Bassiuny, Abdel Ghany M. Abdel Ghany. 2022. "Design Variable Structure Fuzzy Control Based on Deep Neural Network Model for Ser-vomechanism Drive System." International Journal of Power Electronics and Drive Systems (IJPEDS) 13 (4).

[11] Mustafa, Ghazally I.Y., Xinian Li, and Haoping Wang. 2022. "A New Neural

Network-Based Adaptive Time-Delay Control for Nonlinear Car Active Suspension System." Studies in Informatics and Control 31 (4): 13–24.
[12] M. A. Shamseldin, "Design of Auto-Tuning Nonlinear PID Tracking Speed Control for Electric Vehicle with Uncertainty Consideration," World Electr. Veh. J. - MDPI, vol. 14, no. 78, 2023.
[13] Omar, M., M. A. Ebrahim, A. M. AbdelGhany, and F. Bendary. 2016. "Tuning of PID Controller for Load Frequency Control Problem via Harmony Search Algorithm." Indonesian Journal of Electrical Engineering and Computer Science 1 (2): 255–63. https://doi.org/10.11591/ijeecs.v1.i2.pp255-263.
[14] Poovarasan, J, R Kayalvizhi, and R K Pongiannan. 2014. "Design of Fractional Order PID Controller for a CSTR Pro-cess." International Refereed Journal of Engineering and Sci-ence (IRJES) 3 (1): 8–14.
[15] ROMAN, Raul-Cristian, Radu-Emil PRECUP, Emil M. PETRIU, and Mihai MUNTYAN. 2023. "Fictitious Reference Iterative Tuning of Discrete-Time Model-Free Control for Tow-er Crane Systems." Studies in Informatics and Control 32 (1): 5–14. https://doi.org/10.24846/v32i1y202301.
[16] Sauber, Amr M., Mohamed H. Behiry, and Mohamed Amin. 2022. "Real-Time Optimization for an AVR System Using Enhanced Harris Hawk and IIoT." Studies in Informatics and Control 31 (2): 81–94. https://doi.org/10.24846/v31i2y202208.
[17] Shamseldin, Mohamed A. 2023. "Design of Auto-Tuning Non-linear PID Tracking Speed Control for Electric Vehicle with Uncertainty Consideration." World Electric Vehicle Journal - MDPI 14 (78).
[18] SHAMSELDIN, MOHAMED A. 2021. "Optimal Covid-19 Based PD/PID Cascaded Tracking Control for Robot Arm Driven by BLDC Motor." WSEAS TRANSACTIONS on SYSTEMS 20 (1).
[19] Suwarno, Iswanto, Yaya Finayani, Robbi Rahim, Jassim Alhamid, and Ahmed Ramadhan Al-Obaidi. 2022. "Controllability and Observability Analysis of DC Motor System and a Design of FLC-Based Speed Control Algorithm." Journal of Robotics and Control (JRC) 3 (2): 227–35. https://doi.org/10.18196/jrc.v3i2.10741.

Contribution of Individual Authors to the Creation of a Scientific Article (Ghostwriting Policy)

The authors equally contributed in the present research, at all stages from the formulation of the problem to the final findings and solution.

Sources of Funding for Research Presented in a Scientific Article or Scientific Article Itself
No funding was received for conducting this study.

Conflict of Interest
The authors have no conflicts of interest to declare that are relevant to the content of this article.